SLIDING MODE CONTROL OF A 4Y OCTOROTOR

Victor G. ADÎR[1], Adrian M. STOICA[2], James F. WHIDBORNE[3]

Lucrarea prezintă o metodă de control neliniar, mai exact sliding mode, care este aplicată pentru un vehicul octorotor de tip 4Y. Acesta constituie o extensie a popularului model cu patru rotoare. Dublarea numărului de actuatoare poate duce la o creştere a siguranței în exploatare şi a capacității de încărcare. Legile de control pentru stabilizare şi navigație aplicate asupra modelului dinamic neliniar al octorotorului sunt testate cu ajutorul simulărilor numerice. Capabilitatea de respingere a incertitudinii legate de masă este de asemenea investigată.

The paper presents a non-linear control approach, namely sliding mode, which is applied on the 4Y octorotor. This UAV can be regarded as an extension of the popular quadrotor. By adding 4 rotors the reliability and the payload capacity of the vehicle can be increased. Numerical simulations test the stabilization and waypoint navigation controllers applied on the non-linear dynamic model of the 4Y octorotor. The rejection of mass related uncertainty is also investigated.

Keywords: VTOL aircraft, autonomous UAV, octorotor, sliding mode control

1. Introduction

Nowadays, UAVs (unmanned aerial vehicles) are becoming more and more popular. They are used by the military for precise target recognition and destruction. The UAV is an important tool that has shaped the war-time strategies of the army. However, in the recent years the civilian field has also developed a high interest for aerial drones. Most UAVs are based on piloted configurations, one notable exception being the quadrotor. As its name implies, it is powered by four rotors. Unlike conventional helicopters, it has fixed pitch-propellers. Thus control is achieved by varying the speed of the rotors in order to induce the required forces and moments on its body.

Because of its configuration, the quadrotor is capable of VTOL (vertical take-off and landing) and it is highly manoeuvrable. It can be used for monitoring important points of interest (by offering a live video feed, for example), aerial mapping (with applications in landscaping and agriculture), search and rescue operations, law enforcement missions, army ground forces support and a lot more.

[1] PhD, University POLITEHNICA of Bucharest, Romania, e-mail: victor.adir@gmail.com
[2] Prof., University POLITEHNICA of Bucharest, Romania, e-mail: amstoica@rdslink.ro
[3] Senior Lecturer, Cranfield University, United Kingdom, e-mail: j.f.whidborne@cranfield.ac.uk

The propellers can be enclosed in a protective shroud (ducted propellers) not only to increase safety, but also to give the quadrotor the possibility of indoor flight without the risk of causing important damage in the case of a collision. This further expands its range of applications for both outdoor and indoor environments.

A lot of research is taking place in the field of quadrotor development and multiple entities are involved in modelling these vehicles, designing their control laws and implementing them. Major steps have been taken towards autonomous flight, as satellite positioning systems, micro-electro-mechanical (MEMS) systems and control methodologies have evolved.

An important problem of the quadrotor is its lack of redundancy. Even if failure strategies have been developed, the quadrotor still depends on all of the 4 rotors in order to provide full control. If even just one of them is completely inoperative, then stabilization is impossible without reversing the direction of the motor or sacrificing the controllability of the yaw state, as seen in [1]. Research presented in [2], [3] and [4] has shown that some partial failures can be handled, which can occur following collisions where only part of the rotor blade is damaged. However, in practice complete actuator failure can occur as well.

In order to introduce the quadrotors in more and more fields of activity, additional functionality is needed. For example, providing a live video feed requires specific hardware, both for image capturing and transmitting. This adds extra weight to the quadrotor, but its payload is limited.

The present work addresses the payload restrictions of the quadrotor by proposing the use of a 4Y octorotor configuration (see Fig. 1). Also, by introducing the additional 4 rotors an important step in increasing the reliability of the vehicle is taken. The proposed vehicle is made up of 4 Y-shaped arms connected to a central baseplate which holds the battery, control electronics and sensors. Motors are installed at the end of each outboard arm, totalling eight fixed pitch rotors. Depending on the combination of failing rotors, the vehicle can tolerate up to 4 failures (see [5]).

Section 2 introduces the dynamics of the 4Y octorotor along with additional information necessary for this research, like model assumptions and simplifications that reduce the complexity of the problem to that of the quadrotor. Section 3 presents the synthesis of a non-linear control strategy, namely sliding mode control (see [6] and [7]). Controllers for the stabilization of attitude and altitude are devised and waypoint navigation is added on top of this framework. In Section 4 the results from numerical simulations confirm the effectiveness of the proposed control strategy under different conditions. The final section presents conclusions and proposes future improvements.

Fig. 1. The 4Y Octorotor.

2. Dynamics

The dynamics of the 4Y octorotor were derived taking into account the work on quadrotors which is presented in [8]-[12] and [14].

The following assumptions were made:

- the structure is rigid and symmetric
- the centre of gravity lies at the origin of the body axis reference frame
- the inertia matrix is diagonal
- the propellers are rigid
- the thrust is proportional to the square of the speed of the rotor
- the drag is proportional to the square of the speed of the rotor

As in [13], actuator lag is considered negligible.

The 4Y octorotor layout is presented in Fig. 2 along with the conveniently chosen coordinate system. The standard definition of a positive rotation is used: this is defined as a counter-clockwise rotation around the axis as seen from directly in front of the axis line. Two reference frames are used – a body axes frame B fixed at the vehicle's centre of gravity and an earth fixed frame E.

In order to obtain a configuration which is similar to that of the quadrotor the rotors are paired together two by two in the following manner: pair A - 1 with 2 ($\Omega_1 = \Omega_2 = \Omega_A$), pair B - 3 with 4 ($\Omega_3 = \Omega_4 = \Omega_B$), pair C - 5 with 6 ($\Omega_5 = \Omega_6 = \Omega_C$) and pair D - 7 with 8 ($\Omega_7 = \Omega_8 = \Omega_D$). The rotors belonging to the same pair spin at the same speed and have propellers of the same type (either puller or pusher, depending on the direction of rotation).

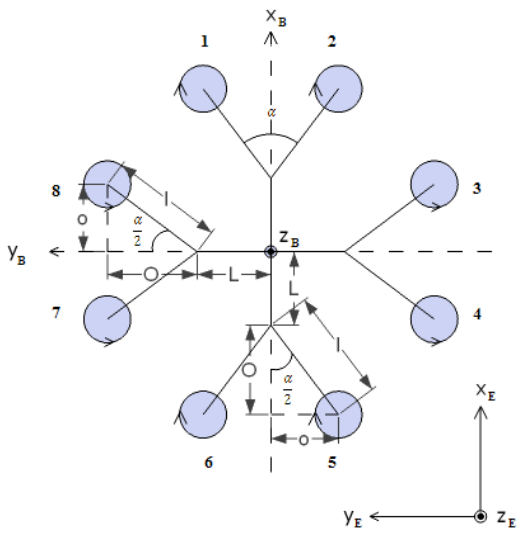

Fig. 2. The 4Y octorotor layout.

To increase the roll angle, the thrust of pair B is decreased while the thrust of pair D is increased such that overall thrust remains the same. To obtain a positive pitch angle, the thrust of pair A is decreased while the thrust of pair C is simultaneously increased. For a positive yaw angle, the speed of the clockwise spinning rotors is increased while the speed of the counter-clockwise ones is decreased. The rotor arrows from Fig. 2 indicate the direction of the resulting torque which is opposite to the direction of rotation.

The control inputs of the system, U_1, U_2, U_3 and U_4, and the disturbance Ω (which depends on the speed of the rotors - Ω_1, Ω_2, Ω_3, Ω_4, Ω_5, Ω_6, Ω_7 and Ω_8) have the following expressions:

$$\begin{cases} U_1 = b[O'(\Omega_7^2 + \Omega_8^2 - \Omega_3^2 - \Omega_4^2) + o(\Omega_1^2 + \Omega_6^2 - \Omega_2^2 - \Omega_5^2)] \\ U_2 = b[O'(\Omega_5^2 + \Omega_6^2 - \Omega_1^2 - \Omega_2^2) + o(\Omega_4^2 + \Omega_7^2 - \Omega_3^2 - \Omega_8^2)] \\ U_3 = d(\Omega_3^2 + \Omega_4^2 + \Omega_7^2 + \Omega_8^2 - \Omega_1^2 - \Omega_2^2 - \Omega_5^2 - \Omega_6^2) \\ U_4 = b(\Omega_1^2 + \Omega_2^2 + \Omega_3^2 + \Omega_4^2 + \Omega_5^2 + \Omega_6^2 + \Omega_7^2 + \Omega_8^2) \\ \Omega = \Omega_3 + \Omega_4 + \Omega_7 + \Omega_8 - \Omega_1 - \Omega_2 - \Omega_5 - \Omega_6 \end{cases}, \quad (1)$$

where:

$$O = l\cos\frac{\alpha}{2}, \quad (2)$$

$$o = l\sin\frac{\alpha}{2}, \quad (3)$$

$$O' = O + L. \quad (4)$$

The outputs of the system are x, y and z - which denote the position of the vehicle with respect to the Earth fixed frame, and p, q and r - which denote the angular velocity of the vehicle with respect to the body fixed frame. The equations describing the dynamics of the 4Y octorotor are (as in the case of the quadrotor modelling presented in [12] and [14]):

$$\begin{cases} \ddot{x} = (cos\,\phi\, sin\,\theta\, cos\,\psi + sin\,\phi\, sin\,\psi)\dfrac{1}{m}U_4 \\ \ddot{y} = (cos\,\phi\, sin\,\theta\, sin\,\psi - sin\,\phi\, cos\,\psi)\dfrac{1}{m}U_4 \\ \ddot{z} = -g + cos\,\phi\, cos\,\theta\dfrac{1}{m}U_4 \\ \dot{p} = qr\left(\dfrac{I_y - I_z}{I_x}\right) - \dfrac{J_r}{I_x}q\Omega + \dfrac{1}{I_x}U_1 \\ \dot{q} = pr\left(\dfrac{I_z - I_x}{I_y}\right) + \dfrac{J_r}{I_y}p\Omega + \dfrac{1}{I_y}U_2 \\ \dot{r} = pq\left(\dfrac{I_x - I_y}{I_z}\right) + \dfrac{1}{I_z}U_3. \end{cases} \tag{5}$$

In order to obtain the angular velocity with respect to the Earth fixed frame the following multiplication is performed (see [15] and [16]):

$$\begin{bmatrix} \dot{\phi} \\ \dot{\theta} \\ \dot{\psi} \end{bmatrix} = \begin{bmatrix} 1 & \sin\phi\tan\theta & \cos\phi\tan\theta \\ 0 & \cos\phi & -\sin\phi \\ 0 & \dfrac{\sin\phi}{\cos\theta} & \dfrac{\cos\phi}{\cos\theta} \end{bmatrix}\begin{bmatrix} p \\ q \\ r \end{bmatrix}. \tag{6}$$

Because of the pairing some of the terms in equation set (1) cancel:

$$\begin{cases} U_1 = b[O'(\Omega_7^2 + \Omega_8^2 - \Omega_3^2 - \Omega_4^2)] \\ U_2 = b[O'(\Omega_5^2 + \Omega_6^2 - \Omega_1^2 - \Omega_2^2)] \\ U_3 = d(\Omega_3^2 + \Omega_4^2 + \Omega_7^2 + \Omega_8^2 - \Omega_1^2 - \Omega_2^2 - \Omega_5^2 - \Omega_6^2) \\ U_4 = b(\Omega_1^2 + \Omega_2^2 + \Omega_3^2 + \Omega_4^2 + \Omega_5^2 + \Omega_6^2 + \Omega_7^2 + \Omega_8^2) \\ \Omega = \Omega_3 + \Omega_4 + \Omega_7 + \Omega_8 - \Omega_1 - \Omega_2 - \Omega_5 - \Omega_6. \end{cases} \tag{7}$$

The inputs of the system become:

$$\begin{cases} U_1 = 2b[O'(\Omega_D^2 - \Omega_B^2)] \\ U_2 = 2b[O'(\Omega_C^2 - \Omega_A^2)] \\ U_3 = 2d(\Omega_B^2 + \Omega_D^2 - \Omega_A^2 - \Omega_C^2) \\ U_4 = 2b(\Omega_A^2 + \Omega_B^2 + \Omega_C^2 + \Omega_D^2). \end{cases} \tag{8}$$

From equation set (8) it follows that:

$$\begin{cases} \Omega_1 = \Omega_2 = \Omega_A = \sqrt{-\dfrac{1}{4bO'}U_2 - \dfrac{1}{8d}U_3 + \dfrac{1}{8b}U_4} \\ \Omega_3 = \Omega_4 = \Omega_B = \sqrt{-\dfrac{1}{4bO'}U_1 + \dfrac{1}{8d}U_3 + \dfrac{1}{8b}U_4} \\ \Omega_5 = \Omega_6 = \Omega_C = \sqrt{\dfrac{1}{4bO'}U_2 - \dfrac{1}{8d}U_3 + \dfrac{1}{8b}U_4} \\ \Omega_7 = \Omega_8 = \Omega_D = \sqrt{\dfrac{1}{4bO'}U_1 + \dfrac{1}{8d}U_3 + \dfrac{1}{8b}U_4}. \end{cases} \tag{9}$$

The nominal parameters of the 4Y octorotor are: $L = 0.158m$ - length of inboard arm, $l = 0.25m$ - length of outboard arm, $\alpha = 78^o$ - angle between outboard arms, $m = 1.56kg$ - mass, $I_x = 0.04kg \cdot m^2$ - inertia on x axis, $I_y = 0.04kg \cdot m^2$ - inertia on y axis, $I_z = 0.08kg \cdot m^2$ - inertia on z axis, $b = 10 \cdot 10^{-6}N \cdot s^2$ - thrust coefficient, $d = 0.3 \cdot 10^{-6}N \cdot m \cdot s^2$ - drag coefficient and $J_r = 90 \cdot 10^{-6}kg \cdot m^2$ - rotor inertia. The maximum rotor thrust that can be achieved is 6.25 N. The gravitational constant g is taken as $9.81m/s^2$.

3. Controller Design

a) Model Simplification

The design process can be simplified by modifying the dynamic model describing the behaviour of the vehicle as follows (see [5] and [8]-[12]):

$$\begin{cases} \ddot{x} = (cos\,\phi\, sin\,\theta\, cos\,\psi + sin\,\phi\, sin\,\psi)\dfrac{1}{m}U_4 \\ \ddot{y} = (cos\,\phi\, sin\,\theta\, sin\,\psi - sin\,\phi\, cos\,\psi)\dfrac{1}{m}U_4 \\ \ddot{z} = -g + cos\,\phi\, cos\,\theta\,\dfrac{1}{m}U_4 \\ \ddot{\phi} = \dot{\theta}\dot{\psi}\left(\dfrac{I_y - I_z}{I_x}\right) - \dfrac{J_r}{I_x}\dot{\theta}\Omega + \dfrac{1}{I_x}U_1 \\ \ddot{\theta} = \dot{\phi}\dot{\psi}\left(\dfrac{I_z - I_x}{I_y}\right) + \dfrac{J_r}{I_y}\dot{\phi}\Omega + \dfrac{1}{I_y}U_2 \\ \ddot{\psi} = \dot{\phi}\dot{\theta}\left(\dfrac{I_x - I_y}{I_z}\right) + \dfrac{1}{I_z}U_3. \end{cases} \tag{10}$$

This is a valid approximation when perturbations from hover flight are small and $(\dot{\phi}, \dot{\theta}, \dot{\psi}) \approx (p, q, r)$. This simplified model suits the purpose and is widely used in different research materials.

Note that the dynamics of the vehicle is simulated using the proper model and considering the true capabilities of the actuators, as saturation may affect the control process. The simplified model described in equation set (10) is only used to design the control laws.

The state vector is chosen as:

$$X^T = [x_1\ x_2\ x_3\ x_4\ x_5\ x_6\ x_7\ x_8\ x_9\ x_{10}\ x_{11}\ x_{12}]^T. \tag{11}$$

More precisely:

$$X^T = \left[x\ \dot{x}\ y\ \dot{y}\ z\ \dot{z}\ \phi\ \dot{\phi}\ \theta\ \dot{\theta}\ \psi\ \dot{\psi}\right]^T. \tag{12}$$

The dynamic model presented in equation set (10) can be written in state space form as:

$$\dot{X} = f(X, U), \tag{13}$$

where:

$$f(X,U) = \begin{cases} x_2 \\ u_x \dfrac{1}{m} U_4 \\ x_4 \\ u_y \dfrac{1}{m} U_4 \\ x_6 \\ -g + cos\, x_7\, cos\, x_9 \dfrac{1}{m} U_4 \\ x_8 \\ x_{10} x_{12} \left(\dfrac{I_y - I_z}{I_x}\right) - \dfrac{J_r}{I_x} x_{10} \Omega + \dfrac{1}{I_x} U_1 \\ x_{10} \\ x_8 x_{12} \left(\dfrac{I_z - I_x}{I_y}\right) + \dfrac{J_r}{I_y} x_8 \Omega + \dfrac{1}{I_y} U_2 \\ x_{12} \\ x_8 x_{10} \left(\dfrac{I_x - I_y}{I_z}\right) + \dfrac{1}{I_z} U_3. \end{cases} \tag{14}$$

and:

$$u_x = cos\, x_7\, sin\, x_9\, cos\, x_{11} + sin\, x_7\, sin\, x_{11}, \tag{15}$$

$$u_y = cos\, x_7\, sin\, x_9\, sin\, x_{11} - sin\, x_7\, cos\, x_{11}. \tag{16}$$

The control variables u_x and u_y can be regarded as virtual commands which rotate the thrust vector U_4 in such a way that the desired $x - y$ translation motion is achieved.

b) Control Law Synthesis

An altitude controller will provide U_4 which dictates overall thrust. The controller for the $x-y$ position will compute the desired roll and pitch angles depending on the desired values for x and y. These angles, along with the desired yaw angle, are fed into the attitude controller which provides U_1, U_2 and U_3.

Because of its disturbance rejection and robustness properties, the sliding mode control has received considerable attention in the non-linear system control literature. The main idea behind the classical sliding mode control is the possibility to keep the system state trajectory on a chosen surface [6] called the sliding surface (or manifold) by using discontinuous control. In [17] and [18] significant developments can be found, including the intensively discussed "control-chattering" issue determined by the variable structure of the controller. In [7] and [11] some applications regarding sliding mode control of aerial vehicles are presented.

The *sign* function, which is used later, is defined as:

$$sign(s_k) = \begin{cases} +1, s_k > 0 \\ 0, s_k = 0 \\ -1, s_k < 0. \end{cases} \quad (17)$$

The equation describing the vertical motion of the 4Y octorotor where the disturbance term d_3 was added is:

$$\dot{x}_6 = -g + cos\, x_7\, cos\, x_9 \frac{1}{m} U_4 + d_3. \quad (18)$$

The altitude tracking error is:

$$e_3 = x_5 - x_{5d} \quad (19)$$

and $s_3 = 0$ is the sliding surface defined as:

$$s_3 = \dot{e}_3 + \alpha_3 e_3, \text{ where } \alpha_3 > 0. \quad (20)$$

Its time derivative is:

$$\dot{s}_3 = \ddot{e}_3 + \alpha_3 \dot{e}_3 = \ddot{x}_5 - \ddot{x}_{5d} + \alpha_3(\dot{x}_5 - \dot{x}_{5d}), \quad (21)$$

which, after replacing $\dot{x}_5$ by x_6 becomes:

$$\dot{s}_3 = -g + cos\, x_7\, cos\, x_9 \frac{1}{m} U_4 + d_3 - \ddot{x}_{5d} + \alpha_3(x_6 - \dot{x}_{5d}). \quad (22)$$

The following Lyapunov function candidate is chosen:

$$V_3 = \frac{1}{2} s_3^2. \quad (23)$$

Its time derivative is:

$$\dot{V}_3 = s_3 \dot{s}_3. \quad (24)$$

Then, for:

$$U_4 = \frac{m}{cos\, x_7\, cos\, x_9} [g + \ddot{x}_{5d} - \alpha_3(x_6 - \dot{x}_{5d}) - k_3 sign(s_3) - l_3 s_3], \quad (25)$$

where $k_3 > 0$ and $l_3 > 0$, it results that:

$$\dot{s}_3 = -k_3 sign(s_3) - l_3 s_3 + d_3 \tag{26}$$

and therefore:

$$\dot{V}_3 = s_3(-k_3 sign(s_3) - l_3 s_3 + d_3). \tag{27}$$

If k_3 is chosen such that:

$$k_3 > \sup_t |d_3(t)| \tag{28}$$

the control U_4 is stabilizing since $\dot{V}_3 < 0$.

A problem with the sliding mode approach is the chattering phenomenon due to the *sign* function in the expression of U_4. To avoid this drawback which can affect the overall performance, this discontinuous function is replaced by a saturation function defined as follows:

$$sat(s_k) = \begin{cases} sign(s_k), |s_k| \geq \rho_k \\ \dfrac{s_k}{\rho_k}, |s_k| < \rho_k, \end{cases} \tag{29}$$

where ρ_k defines a *boundary layer* around the sliding surface s_k. Thus for avoiding chatter the following modified control law is implemented:

$$U_4 = \frac{m}{cos\, x_7\, cos\, x_9}[g + \ddot{x}_{5d} - \alpha_3(x_6 - \dot{x}_{5d}) - k_3 sat(s_3) - l_3 s_3]. \tag{30}$$

In a similar manner, the control laws for $x - y$ translation and attitude are obtained:

$$u_x = \frac{m}{U_4}[\ddot{x}_{1d} - \alpha_1(x_2 - \dot{x}_{1d}) - k_1 sat(s_1) - l_1 s_1], \tag{31}$$

$$u_y = \frac{m}{U_4}[\ddot{x}_{3d} - \alpha_2(x_4 - \dot{x}_{3d}) - k_2 sat(s_2) - l_2 s_2], \tag{32}$$

$$\begin{aligned} U_1 = I_x \Big[& -x_{10}x_{12}\left(\frac{I_y - I_z}{I_x}\right) + \frac{J_r}{I_x}x_{10}\Omega + \ddot{x}_{7d} - \alpha_4(x_8 - \dot{x}_{7d}) \\ & - k_4 sat(s_4) - l_4 s_4 \Big], \end{aligned} \tag{33}$$

$$\begin{aligned} U_2 = I_y \Big[& -x_8 x_{12}\left(\frac{I_z - I_x}{I_y}\right) - \frac{J_r}{I_y}x_8\Omega + \ddot{x}_{9d} - \alpha_5(x_{10} - \dot{x}_{9d}) \\ & - k_5 sat(s_5) - l_5 s_5 \Big], \end{aligned} \tag{34}$$

$$\begin{aligned} U_3 = I_z \Big[& -x_8 x_{10}\left(\frac{I_x - I_y}{I_z}\right) + \ddot{x}_{11d} - \alpha_6(x_{12} - \dot{x}_{11d}) - k_6 sat(s_6) \\ & - l_6 s_6 \Big]. \end{aligned} \tag{35}$$

Usually, there are no additional sensors installed on board of the vehicle that provide a direct value of the speed of each rotor. Thus the terms from equations (33) and (34) relating to Ω can be regarded as disturbances. In this way they can be omitted from the control laws if proper disturbance rejecting values are chosen for the parameters of the controllers (see [19]).

4. Numerical Simulations

The effectiveness of the control laws presented in the previous section is tested in MATLAB/Simulink. In all test scenarios the 4Y octorotor starts from the origin.

In the first case the 4Y octorotor starts from an initial skew of 30 degrees on all three axes. The controllers have to stabilize its attitude and reach an altitude of 20 metres. As seen in Fig. 3, the proposed approach manages to reach the desired state in a quick and precise manner.

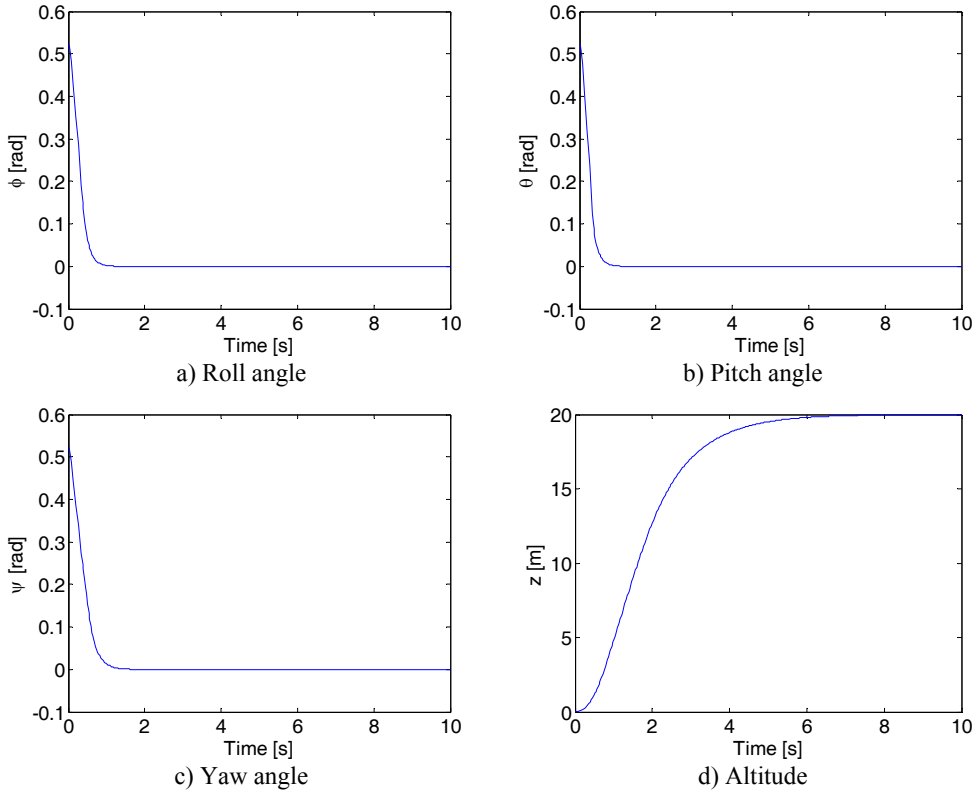

a) Roll angle b) Pitch angle

c) Yaw angle d) Altitude

Fig. 3. Time responses for the first scenario

The second scenario is intended for testing the previously developed waypoint navigation feature of the 4Y octorotor. The desired angles for roll and pitch, which will be fed into the attitude controller, are determined from the virtual commands u_x and u_y. Their expressions are given in (15) and (16). Consider the system comprised of these two equations. If the values of u_x, u_y and ψ are provided, then the two unknown parameters of this system can be

determined. Thus, one obtains the expressions for the desired roll and pitch angles as follows:

$$\phi_d = arcsin\,(\sin\psi\,u_x - \cos\psi\,u_y) \tag{36}$$

$$\theta_d = arcsin\left(\frac{\cos\psi\,u_x + \sin\psi\,u_y}{\cos\phi_d}\right) \tag{37}$$

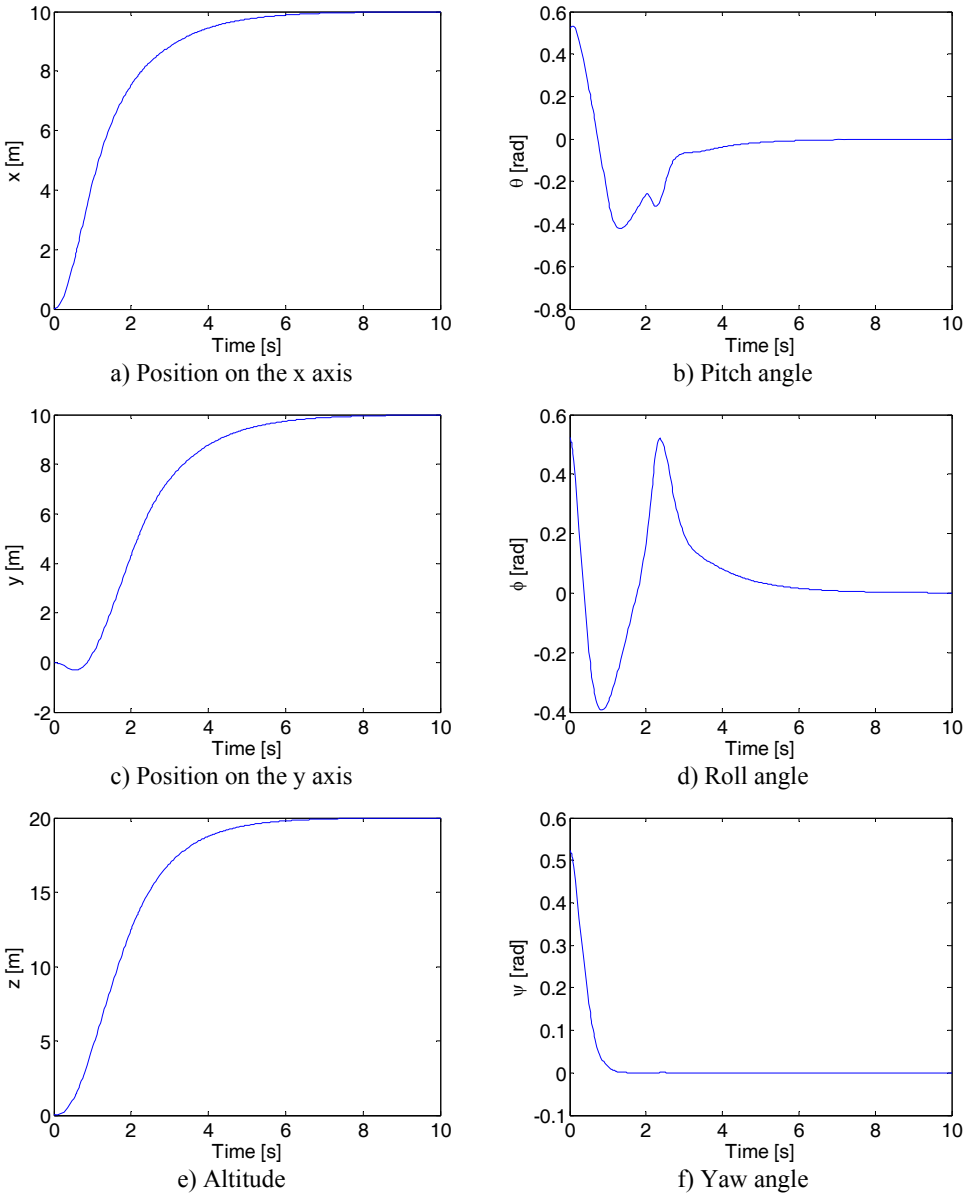

a) Position on the x axis b) Pitch angle

c) Position on the y axis d) Roll angle

e) Altitude f) Yaw angle

Fig. 4. Time responses for the second scenario

Starting from the origin in the same upset configuration used for the first test case, the 4Y octorotor has to reach the position defined by (10,10,20) while maintaining a yaw angle value of 0 degrees. Fig. 4 presents the time responses obtained in this simulation. One observes that the control laws act on the vehicle as intended, thus achieving the desired results.

The third scenario and the fourth scenario investigate the effect of uncertainty in the vehicle mass. This parameter appears in the altitude and $x - y$ translation control laws. These scenarios have been considered in order to test the controller robustness with respect to the variation of mass.

The mass of the vehicle is assumed to be 25 percent lower than its nominal value. Fig. 5 shows that the vehicle manages to stabilize itself with no steady state altitude error.

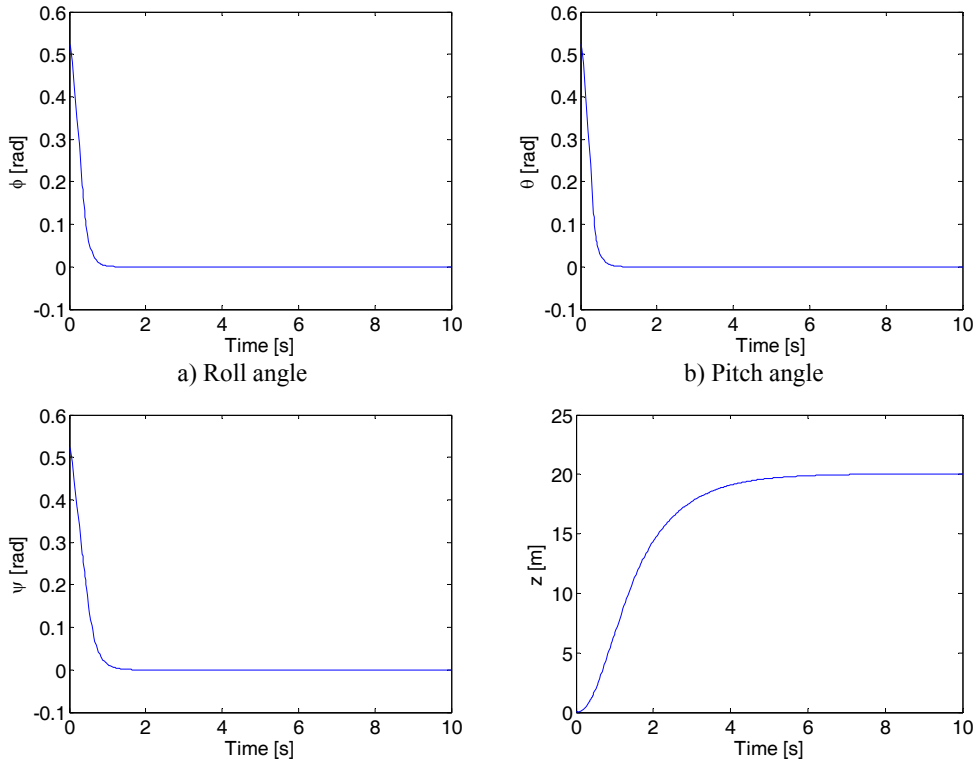

a) Roll angle b) Pitch angle

c) Yaw angle d) Altitude

Fig. 5. Time responses for the third scenario

Afterwards, the mass is considered to be 25 percent greater than its nominal value. The results presented in Fig. 6 confirm that the devised control laws can handle this uncertainty, the vehicle being able to reach the desired waypoint denoted by (10,10,20) while maintaining a stable yaw angle value of 0 degrees.

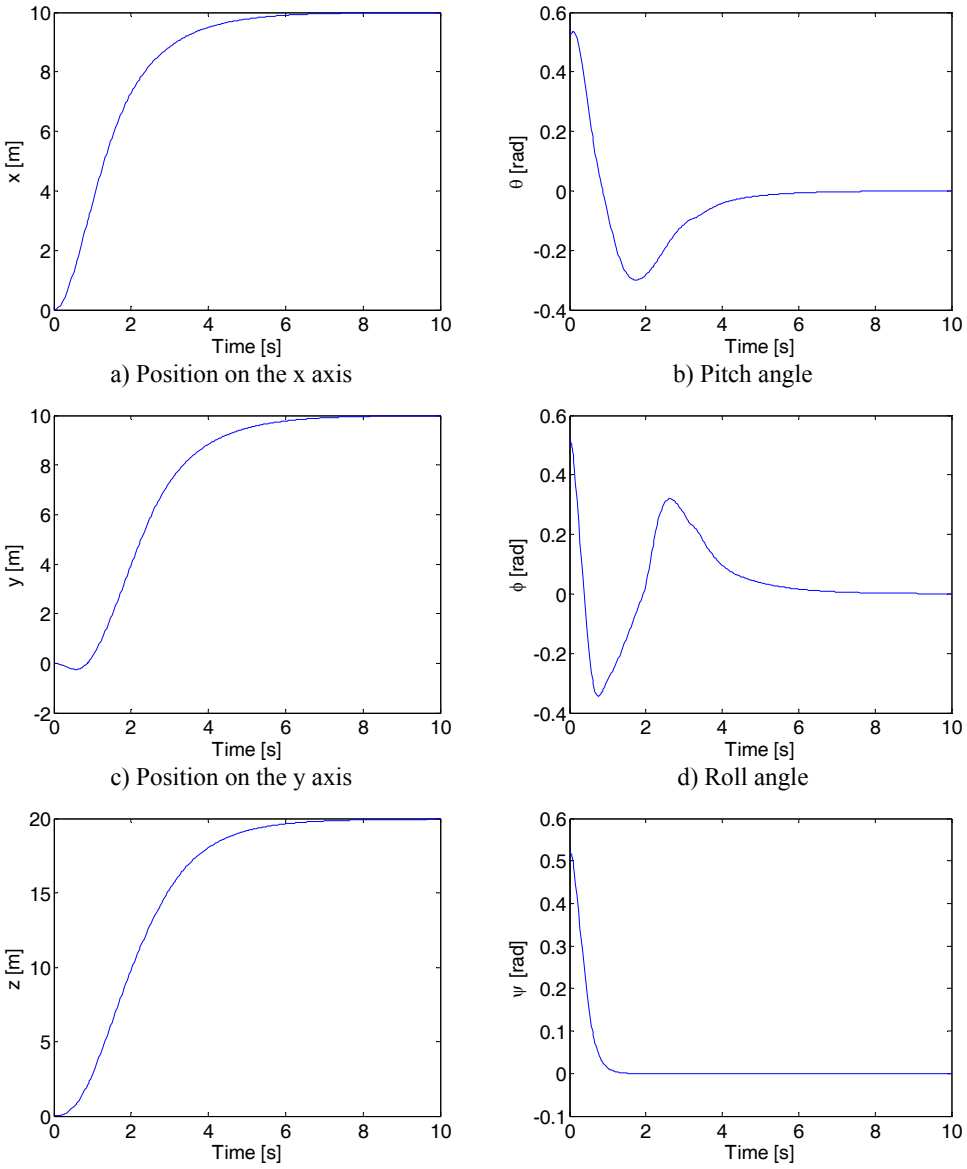

a) Position on the x axis b) Pitch angle

c) Position on the y axis d) Roll angle

e) Altitude f) Yaw angle

Fig. 6. Time responses for the second scenario

In practice, both mass related scenarios are possible. For example, one replaces the battery with a lighter one, resulting in a decrease of overall weight. On the other hand, during specific missions one may wish to add certain sensors or devices to the vehicle, thus increasing the mass of the vehicle. Of course, both

of these situations would result in changing all of the mass related parameters of the 4Y octorotor, like the inertia coefficients I_x, I_y and I_z. However, judging by their magnitude, the mass should have the biggest impact upon the control system.

Table 1

The Parameters of the Control Laws

$x-y$ Translation					
α_1	0.8000	k_1	1.9800	l_1	0.9000
α_2	0.8000	k_2	1.9800	l_2	0.9000
Altitude					
α_3	0.9000	k_3	2.7500	l_3	1.2500
Attitude					
α_4	7.0000	k_4	5.2500	l_4	3.5000
α_5	7.0000	k_5	5.2500	l_5	3.5000
α_6	5.0000	k_6	2.7500	l_6	1.8000

The coefficients of the control laws that were used in the four test scenarios are presented in Table 1.

5. Conclusions and Future Work

The synthesis of sliding mode control laws intended to stabilize the attitude and altitude of the 4Y octorotor was presented. Waypoint navigation controllers were also implemented. These compute the desired values for roll and pitch which are then fed into the attitude controllers in order to achieve $x-y$ translation.

Numerical simulations were carried out on the non-linear dynamic model of the vehicle in order to test the effectiveness of the designed control system. The performance of the chosen approach was demonstrated in multiple test scenarios. Apart from normal operating conditions, two test cases with mass uncertainty were considered. As expected from the sliding mode method, the disturbance was easily rejected by choosing appropriate control parameters.

Future work focuses on another non-linear control technique, namely integral backstepping (see [20] and [21]). The addition of an integral term to the sliding surface as well as other approaches (see [14] and [22]) will also be investigated in order to obtain fault tolerant controllers.

6. Acknowledgements

The work of AUTHOR 1 has been funded by the Sectoral Operational Programme Human Resources Development 2007-2013 of the Romanian Ministry of Labour, Family and Social Protection through the Financial Agreement POSDRU/./..././...

REFERENCES

[1] *Alessandro Freddi, Alexander Lanzon and Sauro Longhi,* "A Feedback Linearization Approach to Fault Tolerance in Quadrotor Vehicles", in Preprints of the 18th IFAC World Congress, Milano (Italy), August 28 - September 2, 2011, pp. 5413-5418

[2] *Tong Li*, Nonlinear and Fault-tolerant Control Techniques for a Quadrotor Unmanned Aerial Vehicle, MSc Thesis, Concordia University, Montreal, 2011

[3] *Alaeddin Bani Milhim*, Modeling and Fault Tolerant PID Control of a Quad-Rotor UAV, MSc Thesis, Concordia University, Montreal, 2010

[4] *Iman Sadeghzadeh, Ankit Mehta, Youmin Zhang and Camille-Alain Rabbath*, "Fault-Tolerant Trajectory Tracking Control of a Quadrotor Helicopter Using Gain-Scheduled PID and Model Reference Adaptive Control", Annual Conference of the Prognostics and Health Management Society, **vol. 2**, 2011

[5] *V. G. Adîr, A. M. Stoica, A. Marks and J. F. Whidborne*, "Modelling, stabilization and single motor failure recovery of a 4Y octorotor", in Proceedings of the IASTED International Conference of Intelligent Systems and Control (ISC 2011), Cambridge, United Kingdom, July 2011, pp. 82 – 87

[6] *V. I. Utkin*, "Variable Structure Systems with Sliding Modes", in IEEE Transactions on Automatic Control, **vol. 22**, 1977, pp. 212-222

[7] *Mehmet Önder Efe*, "Robust Low Altitude Behavior Control of a Quadrotor Rotorcraft Through Sliding Modes", in Proceedings of the 15th Mediterranean Conference on Control & Automation, Athens, Greece, July 2007

[8] *S. Bouabdallah*, Design and Control of Quadrotors with Applications to Autonomous Flying. PhD Thesis, Ecole Polytechnique Federale de Lausanne, 2007

[9] *S. Bouabdallah, P. Murrieri and R. Siegwart*, "Design and control of an indoor micro quadrotor", in Proceedings of the 2004 IEEE International Conference on Robotics and Automation (ICRA '04), **vol. 5**, New Orleans, LA, April 2004, pp. 4393 – 4398

[10] *S. Bouabdallah, A. Noth and R. Siegwart*, "PID vs LQ control techniques applied to an indoor micro quadrotor", in Proceedings of 2004 IEEE/RSJ International Conference on Intelligent Robots and Systems (IROS 2004), **vol. 3**, Sendai, Japan, October 2004, pp. 2451 – 2456

[11] *S. Bouabdallah and R. Siegwart*, "Backstepping and sliding-mode techniques applied to an indoor micro quadrotor", in Proceedings of the 2005 IEEE International Conference on Robotics and Automation (ICRA '05), Barcelona, Spain, April 2005, pp. 2247 – 2252

[12] *Tommaso Bresciani*, Modelling, Identification and Control of a Quadrotor Helicopter, MSc Thesis, Lund University, 2008

[13] *Ian Cowling*, Towards Autonomy of a Quadrotor UAV, PhD Thesis, Cranfield University, 2008

[14] *Youmin Zhang and Abbas Chamseddine*, "Fault Tolerant Flight Control Techniques with Application to a Quadrotor UAV Testbed", Automatic Flight Control Systems - Latest Developments, InTech, January 2012

[15] *Chelaru T.V.*, Dinamica Zborului – Note de curs (Flight Dynamics – Lecture Notes), Editura POLITEHNICA PRESS, Bucureşti, 2009 (in Romanian)

[16] *Guilherme V. Raffo, Manuel G. Ortega and Francisco R. Rubio*, "Backstepping/Nonlinear H∞ Control for Path Tracking of a QuadRotor Unmanned Aerial Vehicle", American Control Conference, Westin Seattle Hotel, USA, June 2008

[17] *V. I. Utkin*, Variable Structure Systems and Sliding Mode - State of the Art Assessment, Variable Structure Control for Robotics and Aerospace Applications, Elsevier, 1993, pp. 9 - 32

[18] *K. D. Young, V. I. Utkin, Ü. Özgüner*, "A Control Engineer's Guide to Sliding Mode Control", in IEEE Transactions on Automatic Control, **vol. 7**, no. 3, 1999, pp. 328-342

[19] *Farid Sharifi, Mostafa Mirzaei, Brandon W. Gordon and Youmin Zhang*, "Fault Tolerant Control of a Quadrotor UAV using Sliding Mode Control", Conference on Control and Fault Tolerant Systems, Nice, France, October 6-8, 2010, pp. 239 – 244

[20] *Roger Skjetne and Thor I. Fossen*, "On Integral Control in Backstepping: Analysis of Different Techniques", in Proceeding of the 2004 American Control Conference, Boston, Massachusetts June 30 - July 2, 2004, pp. 1899 – 1904

[21] *M. Bouchoucha, S. Seghour, H. Osmani and M. Bouri*, "Integral Backstepping for Attitude Tracking of a Quadrotor System", Electronics and Electrical Engineering, **vol. 116**, no. 10, 2011, pp. 75-80

[22] *Kenichiro Nonaka and Hirokazu Sugizaki*, "Integral Sliding Mode Altitude Control for a Small Model Helicopter with Ground Effect Compensation", American Control Conference, San Francisco, CA, USA, June 29 - July 01, 2011, pp. 202 - 207